Received: 23 September 2022 | Accepted: 18 April 2023

DOI: 10.1111/1462-2920.16390

RESEARCH ARTICLE

ENVIRONMENTAL MICROBIOLOGY Applied Microbiology International

Marine *Bacteroidetes* enzymatically digest xylans from terrestrial plants

Theresa Dutschei[1] | **Irena Beidler**[2] | **Daniel Bartosik**[2,3] | **Julia-Maria Seeßelberg**[4] | **Michelle Teune**[1] | **Marcus Bäumgen**[1] | **Soraia Querido Ferreira**[1] | **Julia Heldmann**[1] | **Felix Nagel**[5] | **Joris Krull**[3,6] | **Leona Berndt**[7] | **Karen Methling**[8] | **Martin Hein**[9] | **Dörte Becher**[10] | **Peter Langer**[9] | **Mihaela Delcea**[5] | **Michael Lalk**[8] | **Michael Lammers**[7] | **Matthias Höhne**[4] | **Jan-Hendrik Hehemann**[3,6] | **Thomas Schweder**[2,3] | **Uwe T. Bornscheuer**[1]

[1]Department of Biotechnology & Enzyme Catalysis, Institute of Biochemistry, University Greifswald, Greifswald, Germany

[2]Department of Pharmaceutical Biotechnology, Institute of Pharmacy, University of Greifswald, Greifswald, Germany

[3]Institute of Marine Biotechnology e.V., Greifswald, Germany

[4]Department of Protein Biochemistry, Institute of Biochemistry, University of Greifswald, Greifswald, Germany

[5]Department of Biophysical Chemistry, Institute of Biochemistry, University of Greifswald, Greifswald, Germany

[6]Center for Marine Environmental Sciences, University of Bremen, Bremen, Germany

[7]Department of Synthetic and Structural Biochemistry, Institute of Biochemistry, University of Greifswald, Greifswald, Germany

[8]Department of Cellular Biochemistry and Metabolomics, Institute of Biochemistry, University of Greifswald, Greifswald, Germany

[9]Department of Organic Chemistry, Institute of Chemistry, University of Rostock, Rostock, Germany

[10]Department of Microbial Proteomics, Institute of Microbiology, University of Greifswald, Greifswald, Germany

Correspondence
Thomas Schweder, Department of Pharmaceutical Biotechnology, Institute of Pharmacy, University of Greifswald, 17487 Greifswald, Germany.
Email: schweder@uni-greifswald.de

Uwe T. Bornscheuer, Department of Biotechnology & Enzyme Catalysis, Institute of Biochemistry, University Greifswald, 17487 Greifswald, Germany.
Email: uwe.bornscheuer@uni-greifswald.de

Funding information
German Research Foundation (DFG) "Proteogenomics of Marine Polysaccharide Utilization" (POMPU), Grant/Award Numbers: BO 1862/17-3, HE 7217/2-3, HO 4754/5-2, SCHW 595/10-3

Abstract

Marine *Bacteroidetes* that degrade polysaccharides contribute to carbon cycling in the ocean. Organic matter, including glycans from terrestrial plants, might enter the oceans through rivers. Whether marine bacteria degrade structurally related glycans from diverse sources including terrestrial plants and marine algae was previously unknown. We show that the marine bacterium *Flavimarina* sp. Hel_I_48 encodes two polysaccharide utilization loci (PULs) which degrade xylans from terrestrial plants and marine algae. Biochemical experiments revealed activity and specificity of the encoded xylanases and associated enzymes of these PULs. Proteomics indicated that these genomic regions respond to glucuronoxylans and arabinoxylans. Substrate specificities of key enzymes suggest dedicated metabolic pathways for xylan utilization. Some of the xylanases were active on different xylans with the conserved β-1,4-linked xylose main chain. Enzyme activity was consistent with growth curves showing *Flavimarina* sp. Hel_I_48 uses structurally different xylans. The observed abundance of related xylan-degrading enzyme repertoires in genomes of other marine *Bacteroidetes* indicates similar activities are common in the ocean. The

here presented data show that certain marine bacteria are genetically and biochemically variable enough to access parts of structurally diverse xylans from terrestrial plants as well as from marine algal sources.

INTRODUCTION

Complex carbohydrates photosynthetically produced by marine algae or of terrestrial origin (Field, 1998) can sequester carbon in the ocean (Bligh et al., 2022; Repeta & Aluwihare, 2006). Such polysaccharides are major components of land plants and marine algal biomass (Becker et al., 2020; Kraan, 2012). They serve as intracellular energy storage, structural cell wall components (Kloareg & Quatrano, 1988) and extracellular matrix (Bligh et al., 2022; Hoagland et al., 1993). Many marine bacteria are known to degrade these complex polymeric structures, especially those produced by algae (Arnosti, 2011; Teeling et al., 2012; Yeh & Fuhrman, 2022). Members of the phylum *Bacteroidetes* are selected in such glycan-rich environments (McKee et al., 2021). Recent studies showed the utilization of a diverse range of algal glycans by members of this phylum (e.g., Barbeyron et al., 2016; Beidler et al., 2023; Ficko-Blean et al., 2017; Hehemann et al., 2012; Reisky et al., 2019; Robb et al., 2022; Unfried et al., 2018). Their carbohydrate-active enzymes, or CAZymes, are often co-located with transporters and regulatory proteins in polysaccharide utilization loci (PULs) within bacterial genomes (Martens et al., 2009). CAZymes are specific towards their target polysaccharide and its decorations (Bligh et al., 2022; Hehemann et al., 2014; Reisky et al., 2019), raising the question whether marine bacteria can also degrade glycans from terrestrial plants that reach the ocean.

Rivers transport terrestrial plant-derived organic matter into marine coastal regions (Brockmann, 1994; Herrmann et al., 2016; Opsahl & Benner, 1997; Schefuß et al., 2005). The climate change boosters this carbon input into the ocean by mobilizing soil-bound organic matter (Hemingway et al., 2017). In the Arctic, the warming of permafrost soils leads to an increased mobilization of organic material via river runoff (Peterson et al., 2002; Raymond et al., 2007; Shogren et al., 2021; Tranvik & Jansson, 2002). This export of carbon from land includes material from vascular plants, which contribute unknown quantities of organic carbon to the ocean (Cragg et al., 2020). Glycan structures common in plants, including xylans, have been detected in sediments close to the coast of the Baltic Sea (Salmeán et al., 2022). Xylans and other glycans were also found to sequester carbon in over 1000-year-old sediments (Vidal-Melgosa et al., 2022) of the Red Sea. Presence of xylans in these two different oceanic regions indicates their degradation remains incomplete. Considering that marine bacteria apparently use them as a carbon and energy source, as suggested by import of fluorescent xylans by marine *Bacteroidetes* (D'Ambrosio et al., 2014), and enzymatic degradation of fluorescent xylans added to seawater (Reintjes et al., 2017), this presence of xylans in marine sediments remains puzzling. To resolve the role glycans play for cycling versus sequestration of carbon, different perspectives are required, including biochemical characterization of xylan degrading pathways of marine bacteria.

Terrestrial xylans occur in cell walls of grains and wood in form of arabinoxylan, galactoarabinoxylan and glucuronoxylan sharing a β-1,4-linked D-xylopyranose main chain (Ebringerová, 2005). Besides the combination with other monosaccharides like arabinose, uronic acids and galactose, xylans available in the ocean may also be sulphated, acetylated or phosphorylated. Structural variability remains inaccessible unless bacteria have appropriate enzymes to react (Bäumgen et al., 2021; Deniaud et al., 2003; Hettiarachchi et al., 2019; Hsieh & Harris, 2019; Huang et al., 2021; Viana et al., 2011). It has been shown that xylans are also present in green algae (Chlorophyta/Charophyta) and red algae (Rhodophyta) (Popper et al., 2011). In red macroalgae, like *Palmaria* spp., the backbone is composed of β-1,4- or β-1,3-linked D-xylopyranose, depending on species and source (Hsieh & Harris, 2019; Jensen et al., 2018). β-1,3-xylan structures were found in cell walls of green algae, like *Caulerpa* spp. (Lahaye et al., 2003; Mackie & Percival, 1959). Xylose-containing polysaccharides have also been detected in microalgae (Francis et al., 2021; Huang et al., 2021; Vidal-Melgosa et al., 2021). There are potentially many different, unknown sources of xylans in the coastal ocean.

Their depolymerization requires dedicated enzymatic cascades. Degradation of terrestrial xylans by bacteria has been progressively researched due to its abundance and ecological relevance (Ferreira et al., 1990; Gilbert et al., 1992; Gilbert & Hazlewood, 1993; Gloster et al., 2004; Larsbrink, Rogers, et al., 2014; Larsbrink, Thompson, et al., 2014; Rogowski et al., 2015; Tull & Withers, 1994). This extensive previous work led to the discovery that the marine Bacteroidetes strain *Flavimarina* sp. Hel_I_48 contains two PULs with homologues to xylanases from terrestrial bacteria (PUL I: P162_RS02310-P162_RS02395; PUL II: P162_RS04015-P162_RS04080). These two PULs might provide the ability to consume xylans of unknown origin (Kappelmann et al., 2019). While both PULs share related xylanases and xylosidases of the same

CAZyme family, they differ in some of the associated CAZymes. The two PULs also contain genes for an unusually high number of six different pairs of transporter and receptor proteins for polysaccharide uptake (SusC/D-like pairs).

In this study, we analysed xylan degradation by these two PULs, which are common in other marine *Bacteroidetes* (Krüger et al., 2019). CAZymes and SusD-like binding proteins of these PULs were investigated with four terrestrial and two marine xylans as substrates, covering different xylan structures and common motifs of L-arabinose and D-glucuronic acid decorations. The work shows that marine bacteria can not only consume xylans from algae but also plant xylans that bring terrestrial carbon energy into the ocean.

EXPERIMENTAL PROCEDURES

Bioinformatics and comparative genomics

Databases were created using NCBI RefSeq assemblies (Sayers et al., 2022) of prokaryotic genomes stored in the RefSoilv1 database (Choi, 2017), MarRefv1.7 and MarDBv1.6 (Klemetsen et al., 2018) as well as the NIH Human Microbiome Project (The Human Microbiome Project Consortium, 2012a; The Human Microbiome Project Consortium, 2012b) catalogue with isolation body site 'gastrointestinal_tract'. Genomes were screened for *Flavimarina* sp. Hel_I_48 PUL I- and PUL II-like gene clusters with the 'hmm' search function of cblaster (Gilchrist et al., 2021) v1.3.14 (default settings) using the HMM profiles 'GH67.hmm', 'GH115.hmm', 'CE15.hmm', 'GH43_1.hmm' (all PUL I), 'GH43_10.hmm', 'GH97.hmm', 'GH43_12.hmm', 'CE6.hmm', 'GH8.hmm', 'GH95.hmm' (all PUL II) and 'GH10.hmm' as marker profile from the dbCAN-HMMdb-V10.hmm database (Zhang et al., 2018). CAZyme context of clusters encoding a GH10 with at least two other glycoside hydrolases from PUL I and/or PUL II was predicted using the hmmscan function of HMMer v3.3.2 (Finn et al., 2011) against the dbCAN-HMMdb-V10.hmm database. Hits were filtered using the hmmscan-parser.sh script from dbCAN and validated using Protein–Protein BLAST (v2.11.0+) (Altschul et al., 1997) against CAZyDB (release 09242021) with an e-value threshold of E-20, a minimum sequence identity of 30% and a query coverage of at least 40% (Krüger et al., 2019). The resulting gene clusters were visualized with UpSetR (Conway et al., 2017; Lex et al., 2014) and RIdeogram (Hao et al., 2020). For the phylogenetic tree, *rpoB* genes were aligned using the ClustalW (Thompson et al., 1994) web service in 'slow/accurate' mode and default settings. Maximum-likelihood phylogenies were estimated by the PhyML 3.0 web server (Guindon et al., 2010) with default settings and visualized with iTOL (Letunic & Bork, 2021).

The *Flavimarina* sp. Hel_I_48 PUL repertoire was annotated as described above using additionally the TIGRFAM profile 'TIGR04056.hmm' for prediction of SusC-like proteins and the PFAM models 'PF07980.11.hmm', 'PF12741.7.hmm', 'PF14322.6.hmm' or 'PF12771.7.hmm' for prediction of SusD-like proteins. Final PULs were predicted as described previously (Francis et al., 2021), excluding sulphatase-encoding genes and visualized using Circos (Krzywinski et al., 2009).

Proteome analysis

Flavimarina sp. Hel_I_48 was grown to the late exponential phase in modified MPM medium (Schut et al., 1993) containing 0.1% beechwood xylan (BX), *Palmaria palmata* xylan (PPX), *Caulerpa prolifera* xylan (CPX), rye arabinoxylan (RAX), and wheat arabinoxylan of medium viscosity (WAX-M), insoluble wheat arabinoxylan (WAX-I), or apple pectin (Pec) as sole carbon sources. Triplicates of 50 mL cultures were harvested at 4000 $\times g$, 20 min and 4°C. Cells were resuspended in 50 mM TEAB buffer containing 4% SDS and incubated at 95°C and 600 rpm for 5 min (Thermomixer C, Eppendorf, Hamburg, Germany). Samples were cooled to room temperature before being placed in an ultrasonic bath for 5 min. Cell debris was removed via centrifugation at 14,000 $\times g$ and 4°C for 10 min.

Protein concentration was measured using the BCA Pierce Protein assay kit (Thermo Fisher Scientific Inc., Waltham, MA, USA). Twenty-five microgrammes protein per sample was loaded on a 10% 1D-SDS polyacrylamide gel and separated at 120 V for 90 min. Gels were fixed with a 40% ethanol/10% acetic acid solution and stained overnight using Coomassie G-250 (Candiano et al., 2004). Each sample was divided into 10 subsamples, de-stained using 30% acetonitrile in 200 mM $(NH_4)_2CO_3$ and digested for 16 h using trypsin.

Peptides were separated as described previously (Otto et al., 2010) by reverse phase C18 column chromatography on a nano ACQUITY-UPLC (Waters Corporation, Milford, MA, USA) online-coupled to an LTQ-Orbitrap Classic mass spectrometer (Thermo Fisher Scientific Inc., Waltham, MA, USA). Spectra were searched against a target-decoy protein sequence database including sequences and reverse sequences of *Flavimarina* sp. Hel_I_48 and common laboratory contaminants using MaxQuant (Cox & Mann, 2008). Only proteins that could be detected in at least two out of three replicates were considered identified. Relative protein abundance values in % of all proteins in the same sample were manually calculated from iBAQ values as %riBAQ (relative intensity based absolute quantification). Data and results are available via the PRIDE partner repository (Perez-Riverol et al., 2021) with identifier PXD033600.

Gene cloning and enzyme production

Expression constructs of FI1_GH67, FI2_GH10, FI4_GH10, FI5_hyp, FI7_GH43_1, FI8_CE6 and FI9_hyp (Table S2) were prepared using the FastCloning strategy (primer sequences are listed in Table S3) (Li et al., 2011) with genomic DNA from *Flavimarina* sp. Hel_I_48 as template for the amplification of the inserts. The genomic DNA was extracted as described previously (Chen & Kuo, 1993). The pET28 constructs were prepared as described recently (Reisky et al., 2019).

Escherichia coli BL21(DE3) was transformed with pET28-based plasmids (expression constructs and gene cloning described in the supplementary information) harbouring the required genes. For expression, 50 mL LB or TB medium with 100 μg mL^{-1} kanamycin were inoculated from an overnight culture in LB containing 50 μg mL^{-1} kanamycin. The culture was grown at 37°C and 180 rpm until optical density at 600 nm reached 0.8. Expression was then induced by adding 0.5 or 1 mM isopropyl β-D-1-thiogalactopyranoside (IPTG) and the culture was cooled to 20°C and incubated for 24 h. Enzyme purification is described in the supplementary information.

Plasmids containing the genes encoding for SusD-like proteins were introduced into chemo-competent *E. coli* BL21(DE3) cells. 4 mL of overnight culture in LB media was used to inoculate 600 mL TB media both containing 50 μg mL^{-1} kanamycin. The cells were grown to an optical density at 600 nm (OD_{600}) between 1–1.5 at 37°C and 180 rpm. Temperature was lowered to 20°C and IPTG was added to a final concentration of 1 mM as the OD_{600} reached 2–3. Cells were harvested after 16 h by centrifugation at 4000 ×*g* and 4°C for 20 min including washing with 20 mM sodium phosphate, 500 mM sodium chloride at pH 8. Washed pellets were flash frozen in liquid nitrogen and stored at −20°C until purification. The purification of the SusD-like proteins is described in the supplementary information.

Purification of xylan

Palmaria palmata dulse was purchased at Algenladen (Gießen, Germany). After milling the dry algae (25 g) biomass, it was extracted two times with dH_2O (1 L) for 2 h at 70°C (Deniaud et al., 2003). Afterwards, the solid particles were removed and the water content reduced to a viscous consistency. The polysaccharide was precipitated by adding four volumes of cold ethanol. The precipitate was then separated from the ethanol fraction. Afterwards the alcohol insoluble fraction was dissolved in deionized water and freeze-dried. *Caulerpa prolifera* was extracted with the same protocol. This algal material was provided by the Ozeaneum (Stralsund, Germany). Monosaccharide composition of the self-extracted polysaccharides, charge and size of the used polymers were analysed (Tables S3 and S4). The xylan degradation products from enzymatic reactions and the conversion of purified oligomers were analysed by FACE. Untreated xylan was generally used at a concentration of 1 g L^{-1}, while purified sugar oligomers were used at 0.25 g L^{-1}. Incubation with the enzymes was performed overnight at room temperature. Additional enzymatic assays are described in the supplementary information.

Determination of reducing ends (DNS-assay)

The dinitrosalicylic acid-assay (DNS-assay) was used to determine the reducing ends of the carbohydrates (Bernfeld, 1955). A 20 μL reaction sample of the biocatalysis and 20 μL of the colour reagent were combined and incubated at 100°C for 15 min. After the samples were cooled down to room temperature, 180 μL of water was added, and the 200 μL were transferred to a microtiter plate to measure the absorption at 540 nm in a plate reader (Infinite M200 Pro, Tecan Group, Swiss).

Fluorophore-assisted carbohydrate electrophoresis

Fluorophore-assisted carbohydrate electrophoresis (FACE) was performed with 8-aminonaphthtalene-1,-3,6-trisulphonic acid (ANTS) as fluorophore adapted from Starr et al. (1996). Ten microlitres aliquots of the biocatalysis reaction were lyophilized and dissolved in 4 μL ANTS (0.2 M in water) solution and 4 μL NaCNBH3 (1 M in DMSO) solution. After incubation at 37°C overnight in the dark, the samples were mixed with 20 μL loading buffer and 4 μL were loaded on a FACEgel (Hehemann et al., 2010).

HPLC determination of oligosaccharide degradation products

HPLC analysis for the determination of xylan oligosaccharide standards was performed using a Chrommaster HPLC system from Hitachi (equipped with a Hitachi Chrommaster 5310 column oven) and a detector (Hitachi Chrommaster 5450 RI detector). Analyses were performed with a mobile phase consisting of H_2O with 0.005 M H_2SO_4 on a styrene/polyvinyl benzene copolymer column (SugarSep-H 10 μm 300 × 8 mm) at 70°C for 20 min. The flow rate was set to 0.5 mL min^{-1}.

RESULTS

Flavimarina sp. Hel_I_48 grows on multiple xylans

To test whether *Flavimarina* sp. Hel_I_48 (Figure 1) uses xylans of terrestrial and marine origin, we employed growth experiments and proteomics with different xylans as sole carbon source (Figure S2). We could show that the bacterium is able to grow on different xylans (Figure S1). Proteome analyses showed divergent expression patterns for the two PULs depending on the xylan type. PUL I (P162_RS02310-RS02390) was expressed with beechwood xylan (BX), while PUL II (P162_RS04015-RS04080) remained silent with this substrate (Figure 1). Notably, the expression of SusD_I_2 (P162_RS02355) and SusD_I_3 (P162_RS02370) of PUL I was significantly higher on beechwood xylan compared to the other xylans. SusD_I_3 (P162_RS02370) accounted for 1% of the proteome. This high abundance indicates a specific adaptation of PUL I towards glucuronoxylan, which was recently identified in the coastal ocean with input from the Elbe river (Vidal-Melgosa et al., 2021). In contrast, higher protein levels of SusD_I_1 (P162_RS02310) from PUL I were observed on all investigated xylans, most notably on the marine β-1,4/1,3-mix linked xylan of *P. palmata* (PPX). The broad expression response indicates that this SusD-like protein enables the utilization of the general xylan main-chain structures shared among xylans of different origin. Expression of SusD_II_1 (P162_RS04065) and SusD_II_2 (P162_RS04075) of PUL II was not induced on PPX, BX or *C. prolifera* xylan (CPX), but was high with arabinoxylans from rye (RAX) and wheat (WAX-M) (Figure 1). These xylans contain a β-1,4-xylan main chain with side chains of L-arabinose at the C3 or C2 position (Bastawde, 1992), indicating preference of this PUL region towards such xylans. A separate PUL a with putative arabinofuranosidases (P162_RS00625-RS00655) was significantly upregulated during growth on arabinoxylans compared to the other substrates (Figure 1 and Table S1), which revealed that *Flavimarina* sp. can also consume arabinoxylan. The arabinoxylan was also detected in diatoms (Huang et al., 2021) by using a wheat arabinoxylan-based antibody, which identified xylan in samples of microalgal blooms. Thus, these growth and proteomic data demonstrated that *Flavimarina* sp. is able to access xylans from different sources including algae and terrestrial plants.

SusD-like proteins select diverse xylans

PULs I and II of *Flavimarina* sp. encode six SusD-like proteins that were divergently expressed during growth on different xylan substrates (Figure 1). We investigated the interaction of recombinantly expressed and purified PUL-encoded SusD-like proteins with diverse xylans (BX, PPX, WAX-M, RAX, laminarin and no substrate as controls). SusD-like proteins assist in the transport of glycan oligosaccharides through SusC-like pores into the periplasm (Koropatkin et al., 2008; Pollet et al., 2021). Alternative SusD-like proteins might be required to select for xylan oligosaccharides with different molecular architectures. Affinity gel electrophoresis (Figure S3) showed that SusD_I_2 (P162_RS02355) interacts with glucuronoxylan BX, as it was slower in the electrophoresis with BX. This slower migration correlates with the upregulation observed in the proteome analysis (Figure 1). SusD_I_2 migrated as three bands or as one in the presence of PPX and RAX (Figure S3). These multiple bands, which might represent oligomeric states of the SusD-like proteins, potentially resolved by concentration into one band by the stronger binding of xylan, or xylan types altering oligomerization states (Glenwright et al., 2017; Gray et al., 2021). The absence of detectable interaction with the laminarin control indicates that SusD_I_2 selects for the structure of β-1,4-linked xylan and against other glycans (Figure S3). With increased hydrodynamic diameter of the polymer (BX < WAX-M < RAX < PPX; see Table S5) three bands merged into one as also seen for PPX (Figure S3). In general, ligand size contributes to recognition by SusD-like proteins (Glenwright et al., 2017; Gray et al., 2021). Alpha Fold based structural comparison of SusD_I_2 with its closest characterized homologue, a SusD from *Bacteroides ovatus* (Bacova_02651, PDB 5E76) (Tauzin et al., 2016), revealed a similar overall structure with a sequence identity of 39% (Figure S4A). Previously, Bacova_02651 was shown to bind xyloglucan, structurally related to the glucuronoxylan bound here by SusD_I_2. Comparing binding site hydrophobicity revealed similarities, consistent with SusD_I_2 to select linear conformation xylan with smaller side chains such as glucuronoxylan (Figure S4B). Sequence alignments of the six PUL-encoded SusD-like proteins gave pairwise identities between 19.5% (SusD_II_1 and SusD_II_2) and 27.6% (SusD_I_1 and SusD_I_4) with a high number of gaps (22.6%–39.7%) (Figures S5 and S6). The detected sequence diversity might indicate recognition of different xylan structures by these six SusD-like proteins.

Flavimarina sp. xylanases hydrolyse different xylans

Extracellular enzymes often catalyse initial degradation of polysaccharides into oligosaccharides. Transporters import oligosaccharides for downstream processing through other specialized CAZymes (Arnosti, 2011). We studied the hydrolytic activity of the PUL-encoded

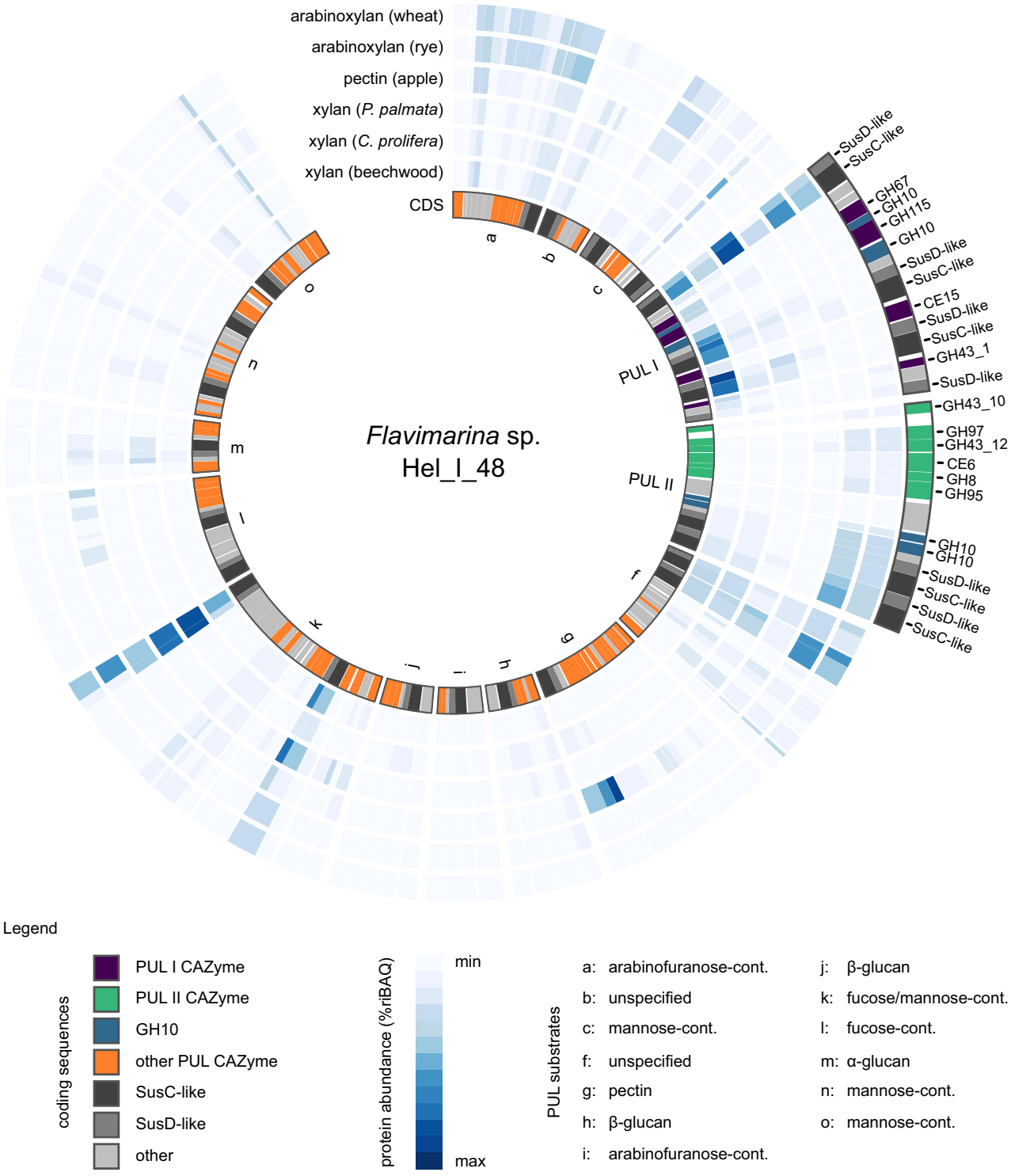

FIGURE 1 PULs and proteomic profiles of *Flavimarina* sp. Hel_I_48. The bacterium was cultivated on different xylose-containing substrates as sole carbon source and with pectin (apple) as control (see Figure S1). Shown are the abundances (%riBAQ) of all PUL-encoded proteins on each substrate (see Table S1) with darker blue colour indicating a higher abundance. Proteins encoded in either of the two xylan-PULs are annotated on the outside of the ring.

enzymes on xylans from different sources (RAX, WAX-M, WAX-I, BX, PPX and β-1,3-linked CPX) using DNS-reducing end assay and fluorophore-assisted carbohydrate electrophoresis (FACE) (Figures S7–S10). Three xylanases contained a lipoprotein signal peptide cleaved by signal peptidase II (Sec/SPII) for extracellular localization on the cell surface (Teufel et al., 2022). FI4_GH10 (P162_RS02345) and FII8_GH10

(P162_RS04060) degraded β-1,4-xylan polymers RAX, WAX-M, WAX-I and BX as well as the β-1,4/1,3 linked PPX (Deniaud et al., 2003; Lahaye et al., 2003), into ladder type oligosaccharides (Figures S7 and S8). This is commonly observed for enzymes with an *endo*-mode of action (Davies & Henrissat, 1995). No activity was observed with the β-1,3-linked CPX. FII7_GH10 (P162_RS04050) was inactive on all xylans. Xylanase activity was detected for FI2_GH10 (P162_RS032335) on RAX, WAX-M, WAX-I, BX and PPX (Figures 2, S7 and S8). FI2_GH10 was inactive on CPX.

FI2_GH10 removed D-xylose and xylobiose (XBI) from xylan-oligosaccharides. Kinetic assisted subside mapping on successively shortened, defined oligosaccharides in conjunction with substrate complex crystal structures and additional experiments would be required to unambiguously ascertain *endo*- or *exo*-mode of action (Figure S11b) (Gilbert, 2010; Gilbert & Hazlewood, 1993; Pell et al., 2004). While FI2_GH10 was able to cleave xylose from arabinoxylo-oligosaccharides with an arabinose substitution in the middle of the oligosaccharide (Figure S11c, XA^3XX), it was inactive on oligosaccharides with arabinose side chain at the non-reducing end (Figure S11c, A^2XX, A^3X).

FI4_GH10 and FII8_GH10 hydrolysed different xylans (Figure S7) potentially explained by the presence of segments of an undecorated β-1,4-xylose main chain in the xylan or the acceptance of decorations in some of the unknown subsites. Acceptance of decorations enables productive binding of different xylans including mixed β-1,4-/1,3-xylans and branches with D-glucuronic acid or L-arabinose, present in BX or arabinoxylans (RAX, WAX-M, WAX-I). Extracellular localization and attachment to the outer membrane, in combination with broad activity shows that *Flavimarina* sp. can access a variety of xylans to extract carbon and energy.

Intracellular enzymatic xylan degradation

The promiscuous extracellular xylanases from both PULs were active on different xylans and deliver the oligosaccharides for the remaining intracellular CAZymes encoded by the two PULs. PUL I encodes two putative

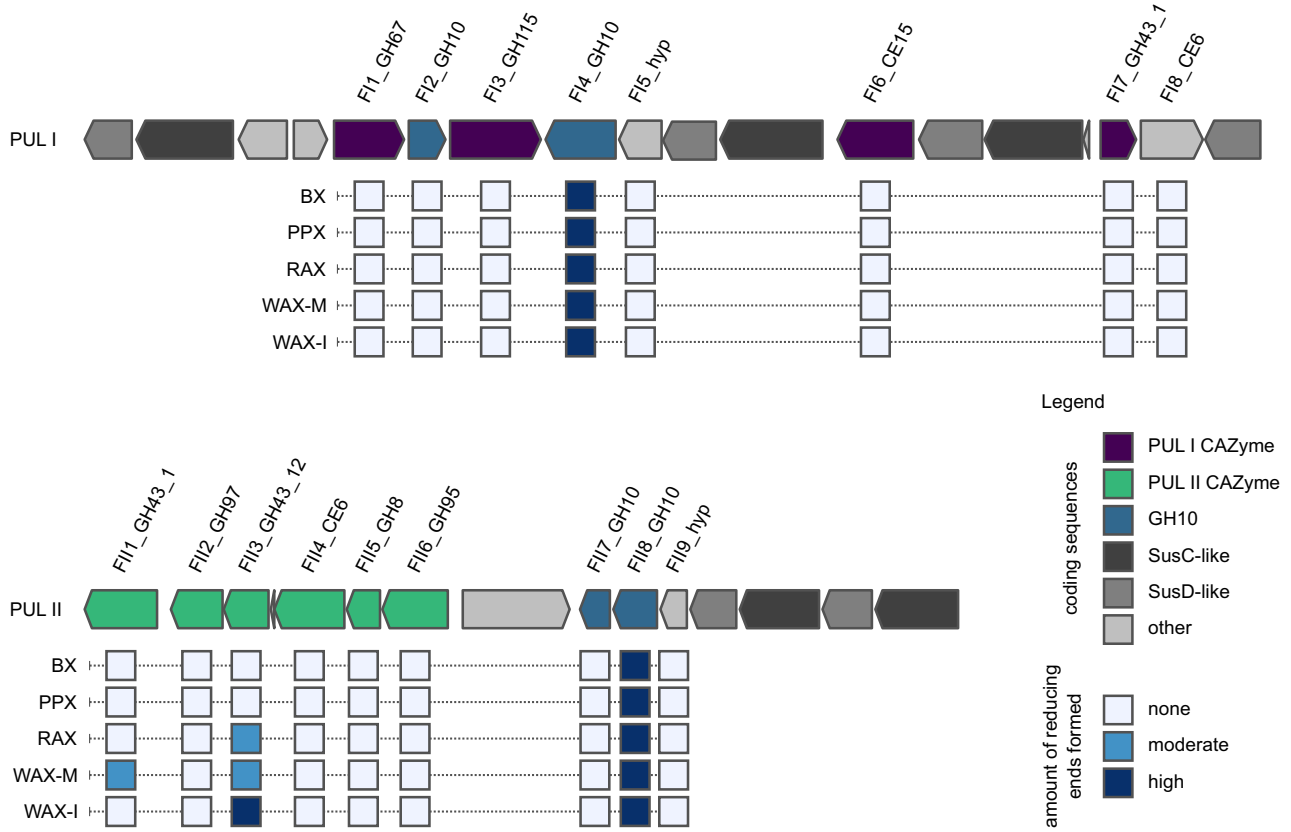

FIGURE 2 PUL organization and initial xylan degradation of *Flavimarina* sp. Hel_I_48. The xylan PULs of *Flavimarina* sp. were defined by Kappelmann et al. (2019). Genome loci refer to the RefSeq assembly (GCF_000733945.1) of PUL I (P162_RS02310-RS02395) and PUL II (P162_RS04015-RS04080). Enzyme activity was determined on the following polysaccharides: beechwood xylan (BX), *Palmaria palmata* xylan (PPX), rye arabinoxylan (RAX), wheat arabinoxylan of medium viscosity (WAX-M) and insoluble wheat arabinoxylan (WAX-I). After incubation, the formed reducing ends were measured using the DNS-reducing end assay (Figure S8). Enzyme activity was designated as moderate when the average absorbance at 540 nm (after subtracting the negative control without enzyme) was between 0.1 and 0.2 and as high for values >0.2.

α-glucuronidases, FI1_GH67 (P162_RS02330) and FI3_GH115 (P162_RS02340), potentially active on glucuronoxylan. Enzymatic assays with *p*NP-α-D-glucuronide showed glucuronidase activity for FI1_GH67 (Figures 3 and S12).

Oligosaccharides made by FI4_GH10, were not active substrates for GHs from PUL I (Figure S9). FII5_GH8 (P162_RS04035) was active on oligosaccharides generated by FII8_GH10 (Figure S10). Combinations of enzymes shifted the bands of BX and PPX derived oligosaccharides to lower molecular size (Figure S13). For RAX, subtle band shifts without intensification of lower molecular weight band were observed. No further activity could be shown on WAX-M and WAX-I. A FACE experiment showed the presence of a band on the same position of the xylose and xylobiose standards. HPLC and TLC revealed that FII5_GH8 removed D-xylose from arabinoxylo-oligosaccharide A^2XX (Figures S11 and S14b).

FII3_GH43 (P162_RS04025), which was upregulated on arabinoxylans, removed L-arabinose from arabinoxylo-oligosaccharides (Figure S14c) and *p*NP-α-L-arabinofuranoside (Figure S12b), in line with a predicted α-L-arabinofuranosidase function. Synthetic substrates revealed further activities of the PUL II-encoded enzyme FII2_GH97, annotated as α-galactosidase (EC.3.2.1.131). FII2_GH97 was active on *p*NP-α-D-galactose (Figure S12c). Terrestrial xylans contain a β-1,4-linked D-xylose main chain with sugar modifications including galactose amounts varying by source (Bastawde, 1992). D-galactose was almost absent in the here investigated xylans (Figure S2), which therefore provided no substrate for FII2_GH97. A compilation of these findings is presented in the xylan degradation scheme in Figure 3.

Carbohydrate esterases increase xylan degradation

Both xylan PULs encode carbohydrate esterases (CE) known to increase the solubility of hemicellulose polymers by cleavage of acetyl groups or phenolic acids. As side groups are removed that cross-link different cell wall polymers, the polysaccharide backbone becomes more accessible to GHs (Hettiarachchi et al., 2019; Williamson et al., 1998).

PUL I encodes FI6_CE15 (P162_RS02365), which was annotated as a CE15, a family containing 4-*O*-methyl-glucuronyl methylesterase activity (Cantarel et al., 2009; Lombard et al., 2014). CE15 enzymes are involved in wood degradation, where they separate hemicelluloses and lignin-like moieties (Charavgi et al., 2013; De Santi et al., 2017). FI6_CE15 was active on the model substrates *p*NP-acetate (Figure S12a), benzyl-D-glucuronic acid and allyl-D-glucuronic acid (Figure S15c). Also, in the ocean this enzyme might cleave methyl esters opening access for CAZymes to the xylan structure. The additional CBM9 domain of FI6_CE15 (Table S2), which is described as a xylan-targeting domain for birch and beechwood xylan, could aid in binding of the polysaccharide. CBM9 family modules can bind insoluble xylan polysaccharides and amorphous or crystalline cellulose (Boraston et al., 2004; Notenboom et al., 2001). PUL I contains one additional carbohydrate esterase, FI8_CE6 (P162_RS02385), which is a CE6 acetyl xylan esterase (Cantarel et al., 2009; Lombard et al., 2014). Deacetylase activity was shown by removal of *O*-acetylation from 6-*O*-acetyl-D-glucose and 6-*O*-acetyl-D-galactose detected with NMR-spectroscopy and an acetate assay (Figure S15b). These two esterase activities from PUL I might be relevant in the degradation of glucuronoxylans. Hardwood xylans contain D-glucuronic acid side groups with methyl and acetylation of the β-1,4-linked D-xylose backbone (Kmezik et al., 2021).

PUL II contains two multimodular esterases, FII1_GH43_10 (P162_RS04015) and FII4_CE6 (P162_RS04030). FII1_GH43_10 consists of a putative acetyl xylan esterase CE3 domain, and an additional GH43_10 module, which is annotated as a xylan β-1,-4-xylosidase/α-L-arabinofuranosidase (Cantarel et al., 2009; Lombard et al., 2014). This domain combination is similar to an enzyme described in *Bacteroides eggerthii*, containing an esterase and a GH43 domain involved in arabinoxylan degradation (Pereira et al., 2021). The putative CE3 and GH43_10 domains were separately analysed here as FII1A_CEnc and FII1B_GH43_10 constructs. Only FII1B_GH43_10 showed xylosidase activity in ANTS-FACE analysis (Figure S9) and a DNS-assay (Figure 2), but no esterase activity was found for FII1A_CEnc.

FII4_CE6 is an enzyme with two CE domains, a CE6/acetyl xylan esterase and an uncharacterized carbohydrate esterase module CEnc, which is likely to be a CE1/feruloyl esterase (Table S2) (Cantarel et al., 2009; Lombard et al., 2014). Ferulic acid xylan esterases target phenolic groups bound to the L-arabinose moieties in arabinoxylans, which enables α-L-arabinofuranosidases to further degrade these polysaccharides (Pereira et al., 2021). This activity was very likely supported by the substantial amounts of ferulic acid released from WAX-I (Figure S15d). FII4_CE6 also showed activity towards *p*NP-acetate and released acetate from partially acetylated birchwood xylan (Figure S15a). A related multimodular CE6|CE1 protein was found in *Bacteroides intestinalis* and was described with a similar activity profile (Pereira et al., 2021). Both CE activities indicate removal of phenolic esters and acetylations, enabling PUL II to potentially use arabinoxylans with such modifications. The PUL-encoded esterases indicate that xylans targeted by *Flavimarina* sp. Hel_I_48 might include acetylations detected in macroalgal polysaccharides (Wong et al., 2021).

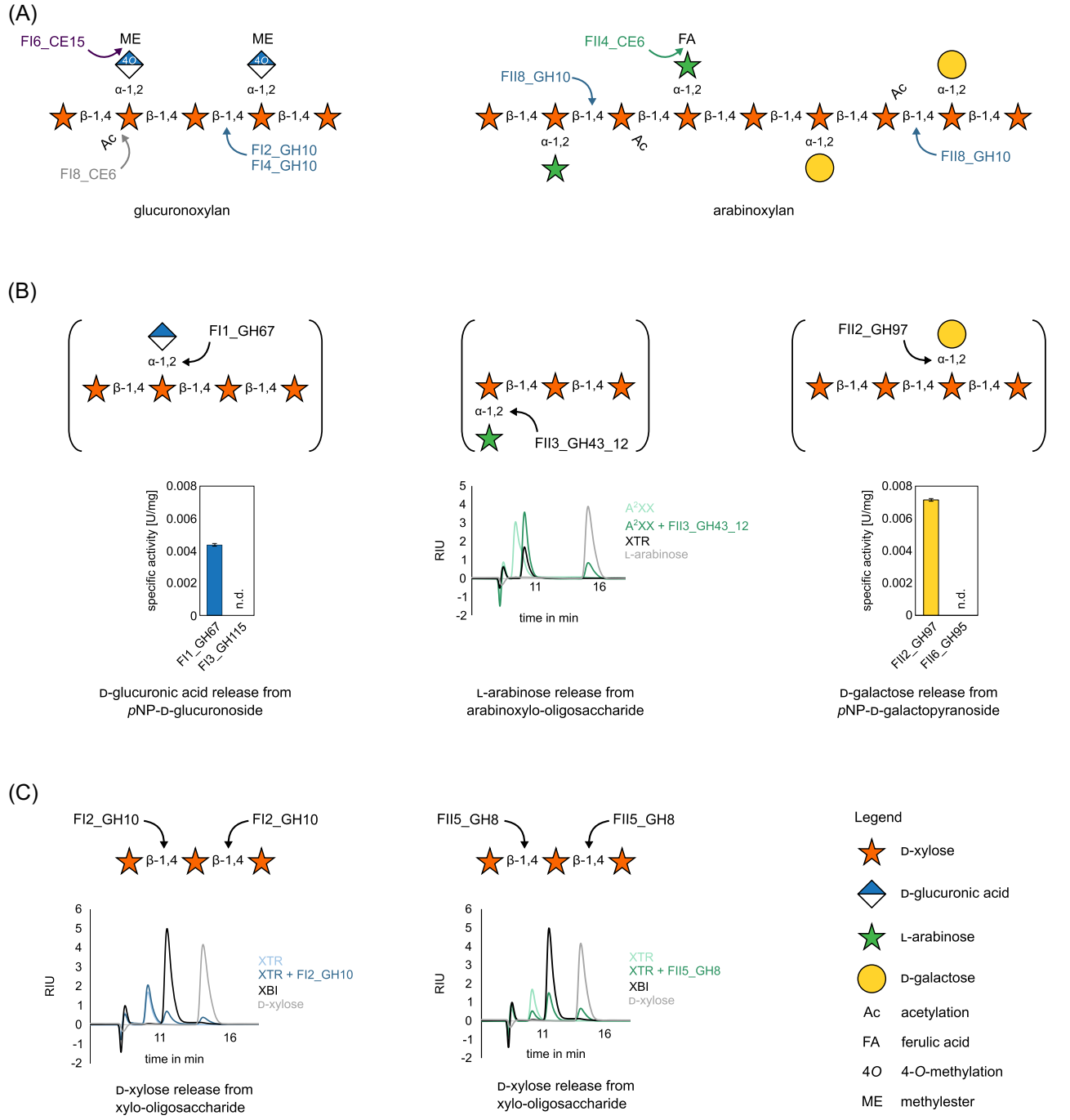

FIGURE 3 Putative enzymatic cascade for the degradation of divergent xylan substrates by PUL I- and PUL II-encoded CAZymes. The targeted structures are assumed to be similar to glucuronoxylan (PUL I) and arabinoxylan (PUL II). Summarized initial degradation (A) of polysaccharides by GH10 xylanases (FI2_GH10, FI4_GH10 and FII8_GH10 (Figure S7), esterase FI8_CE6 cleaving acetate moieties (Figure S15b), FII4_CE6 cleaving acetate and ferulic acid moieties (Figure S15a,d) and FI6_CE15 cleaving 4-*O*-methyl-glucuronyl methyl esters (violet arrow; Figure S15c). The resulting xylo-oligosaccharides can be further digested by other PUL-encoded enzymes, which was investigated using not only the degradation products but also artificial substrates (B). Representatively shown is the release of glucuronic acid (FI1_GH67; Figure S14d) and galactose (FII2_GH97; Figure S14c) from *p*NP-derivates, while arabinose release from artificial oligos was detected upon digestion with FII3_GH43_12 (Figures S11c and S14b). Lastly the undecorated xylo-oligosaccharides can be further degraded (C) by xylosidase-activity detected for e.g. FI2_GH10 and FII5_GH8 (Figure S13b). A^2XX, 2^3-α-L-arabinofuranosyl-xylotriose; XBI, xylobiose; XTR, xylotriose.

Ecological relevance of the xylan degradation pathways and PUL-architecture

Flavimarina sp. degrades a multitude of xylans. This ability is largely facilitated by the broad activity of multiple PUL-associated GH10s on different xylan main chains containing various modifications. A GH10 with additional processing enzymes is likely required for degradation of complex xylans. We identified 226 PULs in marine, terrestrial and human digestive system-associated databases, sharing at least one GH10 and

two additional CAZymes with either of the *Flavimarina* sp. PULs, indicating that complex xylans are important for diverse marine habitats (Figure S16). A modularity search revealed 81 different xylan-PUL architectures, most commonly containing only a few shared enzymes with *Flavimarina* sp. (Figure 4A). The most widely distributed PUL group contains only the enzymes known from *Flavimarina* sp. PUL I, which are GH43 and GH67 alongside a GH10 hydrolase. This enzyme combination was invariable and therefore the core of CAZymes required for xylan degradation. In some cases, bacteria containing such a PUL also contain a second, more complex PUL, such as the terrestrial bacterium *Flavobacterium johnsoniae*, which likely facilitates niche-specific adaptations (Figure 4B).

PUL sequence diversity points towards the ability to degrade different xylan structures that requires specific CAZyme repertoires. Most identified PULs showed no distinct separation between CAZymes homologous to *Flavimarina* sp. PUL I and PUL II. In fact, *Fibrisoma limi* and *Fibrella aestuarina*, the only other species shown to have two enlarged *Flavimarina*-like PULs, are also associated with marine coastal ecosystems (Figure 4B). Some marine bacteria as well as human gut symbionts possess the entire CAZyme spectrum of the *Flavimarina* sp. PULs consolidated into a single PUL (Figure 4B), underlining that similar xylans are carbon sources for microbes from different ecosystems. Notably, many of the related PULs also encode additional CAZymes associated with arabinose-containing polysaccharide degradation, including GH39, GH51 or GH146. *Flavimarina* sp. does not encode CAZymes of these families within its two main xylan-targeting PULs. Some of these GHs are encoded in the genome and associated with the arabinofuranosidase-containing PUL a that was specifically upregulated during growth on RAX and WAX (Figure 1). These observations further indicate that *Flavimarina* sp. has the genetic potential to degrade structurally diverse xylans from different sources available in the dynamic marine land interface of the coastal ocean.

DISCUSSION

This study explores xylan-specific metabolic pathways of a marine *Bacteroidetes* strain. *Flavimarina* sp. Hel_I_48 contains two separate xylan PULs, active on glucuronoxylans (PUL I) and arabinoxylans (PUL II) with similarities to PULs of human gut bacteria and soil bacteria (Pell et al., 2004).

The general occurrence and abundance of xylan PULs in *Bacteroidetes* was previously described for gut microbiota (Rogowski et al., 2015), and xylan degradation was shown for enzymes of microbes from many different environments (Gilbert & Hazlewood, 1993). For example, the gut bacterium *B. ovatus* contains two xylan-targeting PULs (Rogowski et al., 2015), which encode CAZymes showing partially related activities to enzymes of *Flavimarina* sp. Hel_I_48. Our systematic biochemical analysis of PUL-encoded enzymes revealed promiscuous extracellular xylanases, which are active on diverse xylans and generate dedicated oligomers (Pell et al., 2004). An overview of the putative enzymatic cascade for xylan degradation in *Flavimarina* sp. Hel_I_48 is depicted in Figure 3. It is illustrated that these distinct oligosaccharides are further degraded by more specialized intracellular carbohydrate esterases, which remove acetylations and phenolic esters (Figure 3). These enzymatic activities are supported by arabinofuranosidases and glucuronidases, which hydrolyse L-arabinose- and D-glucuronic acid-containing xylans.

Xylans used for the characterization of *Flavimarina* sp. Hel_I_48 PUL-encoded enzymes were from terrestrial plants and marine macroalgae covering structures from both ecosystems and providing a spectrum of xylan structures potentially available in marine habitats. The fact that not all of the PUL-encoded enzymes were found to be active in this study is to be expected, because we are missing xylan substrates from unknown sources. The extent of the potential xylan structure diversity space is likely proportional to the number of species that synthesize xylans and remains to be uncovered. The strain *Flavimarina* sp. Hel_I_48 was isolated during a phytoplankton bloom in the North Sea (Kappelmann et al., 2019) near the island Helgoland, which is close to the river mouth of the Elbe, Germany's largest river that brings terrestrial organic matter into the ocean. Utilization of terrestrial organic matter, including carbohydrates that enter the ocean through rivers (Brockmann, 1994; Schefuß et al., 2005) appears to be a selected strategy for the here tested bacterium. This assumption is supported by the detection of two other putative xylan-utilizing bacteria from marine coastal habitats, *F. limi* (Filippini, Kaech, et al., 2011) and *F. aestuarina* (Filippini, Svercel, et al., 2011), which share the same two enlarged *Flavimarina* sp. PUL architectures (see Figure 4). The lack of sulphatase-encoding genes in these xylan-specific PULs of marine *Bacteroidetes* is another indication that they preferentially target terrestrial-like xylan structures. The simultaneous utilization of macroalgal and terrestrial xylans by these marine PULs might be explained by conserved xylan structures with similar linkages and modifications present in marine algae and terrestrial plants (Hsieh & Harris, 2019; Martone et al., 2009).

The comparative analysis of available *Bacteroidetes* genomes demonstrates that xylan utilization is ecologically relevant in marine habitats and ensured by conserved sets of related xylan-degrading enzymes (Figures 4 and S16). The documented functional activity of xylan utilization from the North Sea isolate

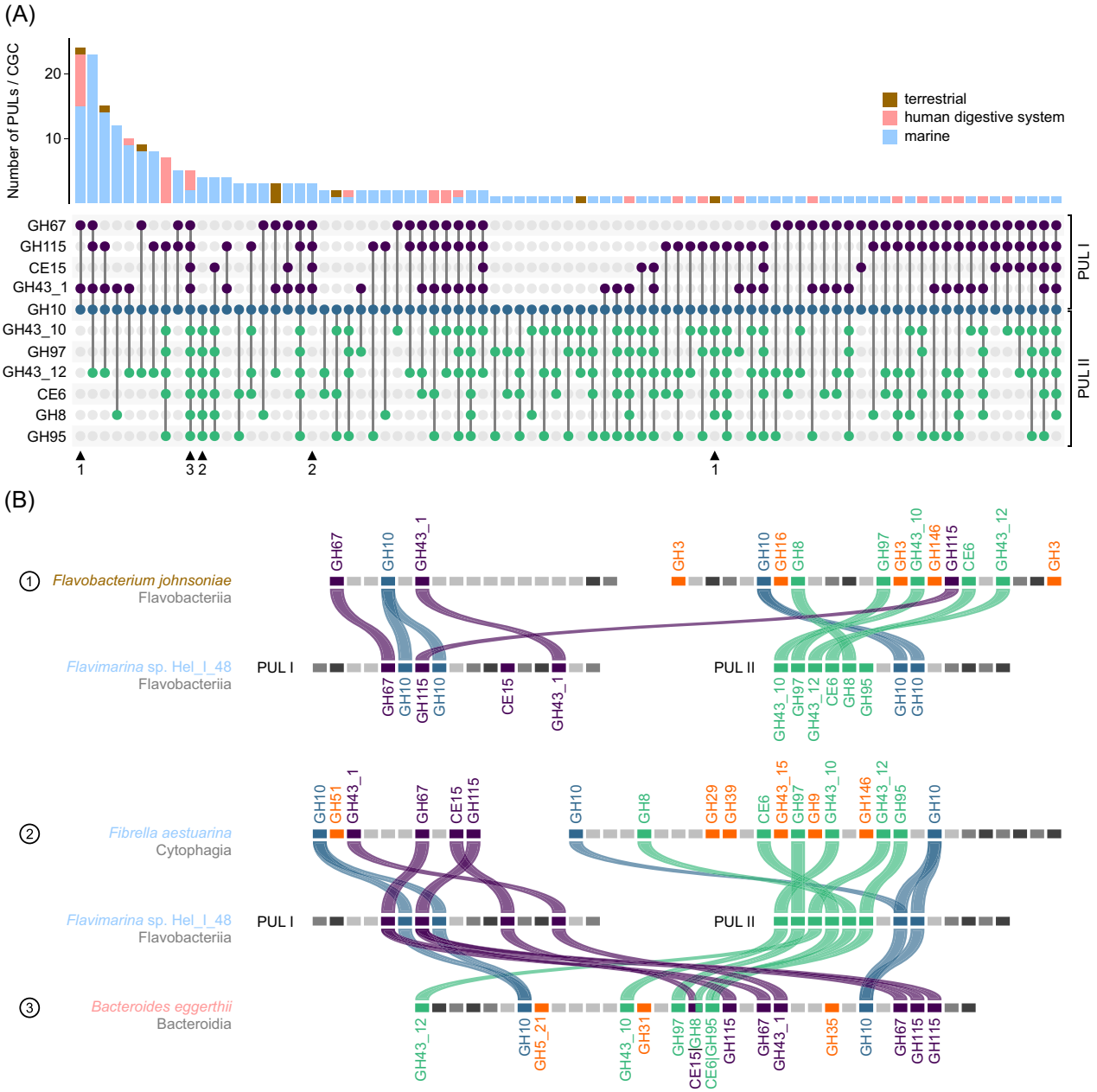

FIGURE 4 Xylan PUL modularity of bacteria from different environments. (A) Upset plot showing different xylan PUL compositions as well as their prevalence in different habitats. (B) Comparison of *Flavimarina* sp. PULs to other significant cluster types, such as those (1) containing a second, more complex PUL, (2) all CAZymes also encoded by *Flavimarina* sp. or (3) all CAZymes but encoded in a single larger PUL. CAZymes of *Flavimarina* sp. PUL I are depicted in purple, those of PUL II in green. CAZymes of families or subfamilies not encoded by either of the *Flavimarina* sp. PULs are marked in orange. See also the complementary phylogenetic tree in Figure S16 of the supplementary information.

Flavimarina sp. indicates that coastal habitats might provide heterogenous xylans with glucurono- and arabino-side groups and acetylation. Marine bacteria that can degrade such xylans from marine algae and terrestrial plants are adapted to access temporally dynamic sources of organic matter in the costal ocean. Their ability to degrade xylans contributes to the unknown magnitude of cycling or sequestration of this type of carbon.

AUTHOR CONTRIBUTIONS

Thomas Schweder: Conceptualization (equal); funding acquisition (equal); project administration (equal); resources (equal); supervision (equal); validation (equal); writing – review and editing (equal). **Theresa Dutschei:** Formal analysis (equal); investigation (equal); methodology (equal); writing – original draft (equal). **Irena Beidler:** Data curation (equal); formal analysis (equal); investigation (equal); methodology

(equal); visualization (equal); writing – review and editing (equal). **Daniel Bartosik:** Data curation (equal); formal analysis (equal); investigation (equal); software (equal); visualization (equal). **Julia-Maria Seeßelberg:** Formal analysis (equal); investigation (equal); methodology (equal). **Michelle Teune:** Data curation (equal); formal analysis (equal); investigation (equal); methodology (equal); writing – review and editing (equal). **Marcus Bäumgen:** Formal analysis (equal); investigation (equal). **Soraia Querido:** Formal analysis (equal); investigation (equal). **Julia Heldmann:** Formal analysis (equal); investigation (equal). **Felix Nagel:** Formal analysis (equal); investigation (equal). **Joris Krull:** Formal analysis (equal); investigation (equal); methodology (equal). **Leona Berndt:** Formal analysis (equal); investigation (equal). **Karen Methling:** Formal analysis (equal); investigation (equal); methodology (equal). **Martin Hein:** Formal analysis (equal); investigation (equal). **Dörte Becher:** Funding acquisition (equal); methodology (equal); resources (equal). **Peter Langer:** Formal analysis (equal); investigation (equal); methodology (equal). **Mihaela Delcea:** Methodology (equal); resources (equal). **Michael Lalk:** Data curation (equal); investigation (equal); methodology (equal). **Michael Lammers:** Investigation (equal); methodology (equal). **Matthias Höhne:** Funding acquisition (equal); investigation (equal); methodology (equal); resources (equal). **Jan Hendrik Hehemann:** Funding acquisition (equal); investigation (equal); methodology (equal); resources (equal); writing – review and editing (equal). **Uwe T. Bornscheuer:** Conceptualization (equal); funding acquisition (equal); project administration (equal); resources (equal); writing – review and editing (equal).

ACKNOWLEDGEMENTS

We thank the German Research Foundation (DFG) for funding through the Research Unit FOR 2406 'Proteogenomics of Marine Polysaccharide Utilization' (POMPU) by grants to Uwe T. Bornscheuer (BO 1862/17-3), Jan-Hendrik Hehemann (HE 7217/2-3), Matthias Höhne (HO 4754/5-2), and Thomas Schweder (SCHW 595/10-3). We are grateful to the Ozeaneum Stralsund, which kindly provided the *C. prolifera* algal biomasses. Open Access funding enabled and organized by Projekt DEAL.

CONFLICT OF INTEREST STATEMENT

The authors declare no conflicts of interest.

DATA AVAILABILITY STATEMENT

The data that support the findings of this study are openly available via the PRIDE partner repository (Perez-Riverol et al., 2021) with identifier PXD033600.

ORCID

Theresa Dutschei https://orcid.org/0000-0003-3053-9536
Julia-Maria Seeßelberg https://orcid.org/0000-0002-5513-6760
Michelle Teune https://orcid.org/0000-0002-0190-6731
Matthias Höhne https://orcid.org/0000-0002-2542-725X
Thomas Schweder https://orcid.org/0000-0002-7213-3596

REFERENCES

Altschul, S.F., Madden, T.L., Schäffer, A.A., Zhang, J., Zhang, Z., Miller, W. et al. (1997) Gapped BLAST and PSI-BLAST: a new generation of protein database search programs. *Nucleic Acids Research*, 25, 3389–3402.

Arnosti, C. (2011) Microbial extracellular enzymes and the marine carbon cycle. *Annual Review of Marine Science*, 3, 401–425.

Barbeyron, T., Thomas, F., Barbe, V., Teeling, H., Schenowitz, C., Dossat, C. et al. (2016) Habitat and taxon as driving forces of carbohydrate catabolism in marine heterotrophic bacteria: example of the model algae-associated bacterium *Zobellia galactanivorans* Dsij^{T}: complete genome of *Zobellia galactanivorans*. *Environmental Microbiology*, 18, 4610–4627.

Bastawde, K.B. (1992) Xylan structure, microbial xylanases, and their mode of action. *World Journal of Microbiology and Biotechnology*, 8, 353–368.

Bäumgen, M., Dutschei, T. & Bornscheuer, U.T. (2021) Marine polysaccharides: occurrence, enzymatic degradation and utilization. *Chembiochem*, 22, 2247–2256.

Becker, S., Tebben, J., Coffinet, S., Wiltshire, K., Iversen, M.H., Harder, T. et al. (2020) Laminarin is a major molecule in the marine carbon cycle. *Proceedings of the National Academy of Sciences*, 117, 6599–6607.

Beidler, I., Robb, C.S., Vidal-Melgosa, S., Zühlke, M.-K., Bartosik, D., Solanki, V. et al. (2023) Marine bacteroidetes use a conserved enzymatic cascade to digest diatom β-mannan. *The ISME Journal*, 17, 276–285.

Bernfeld, P. (1955) Amylases, α and β. In: *Methods in enzymology*. Cambridge: Academic Press, pp. 149–158.

Bligh, M., Nguyen, N., Buck-Wiese, H., Vidal-Melgosa, S. & Hehemann, J.-H. (2022) Structures and functions of algal glycans shape their capacity to sequester carbon in the ocean. *Current Opinion in Chemical Biology*, 71, 102204.

Boraston, A.B., Bolam, D.N., Gilbert, H.J. & Davies, G.J. (2004) Carbohydrate-binding modules: fine-tuning polysaccharide recognition. *The Biochemical Journal*, 382, 769–781.

Brockmann, U.H. (1994) Organic matter in the Elbe estuary. *Netherlands Journal of Aquatic Ecology*, 28, 371–381.

Candiano, G., Bruschi, M., Musante, L., Santucci, L., Ghiggeri, G.M., Carnemolla, B. et al. (2004) Blue silver: a very sensitive colloidal Coomassie G-250 staining for proteome analysis. *Electrophoresis*, 25, 1327–1333.

Cantarel, B.L., Coutinho, P.M., Rancurel, C., Bernard, T., Lombard, V. & Henrissat, B. (2009) The carbohydrate-active enzymes database (CAZy): an expert resource for glycogenomics. *Nucleic Acids Research*, 37, D233–D238.

Charavgi, M.D., Dimarogona, M., Topakas, E., Christakopoulos, P. & Chrysina, E.D. (2013) The structure of a novel glucuronoyl esterase from *Myceliophthora thermophila* gives new insights into its role as a potential biocatalyst. *Acta Crystallographica. Section D, Biological Crystallography*, 69, 63–73.

Chen, W.P. & Kuo, T.T. (1993) Genomic DNA isolation from EPS-producing gram negative bacteria. *Nucleic Acids Research*, 21, 2260.

Choi, J. (2017) *RefSoil database*. figshare. 4477985690 Bytes.

Conway, J.R., Lex, A. & Gehlenborg, N. (2017) UpSetR: an R package for the visualization of intersecting sets and their properties. *Bioinformatics*, 33, 2938–2940.

Cox, J. & Mann, M. (2008) MaxQuant enables high peptide identification rates, individualized p.p.b.-range mass accuracies and

proteome-wide protein quantification. *Nature Biotechnology*, 26, 1367–1372.

Cragg, S.M., Friess, D.A., Gillis, L.G., Trevathan-Tackett, S.M., Terrett, O.M., Watts, J.E.M. et al. (2020) Vascular plants are globally significant contributors to marine carbon fluxes and sinks. *Annual Review of Marine Science*, 12, 469–497.

D'Ambrosio, L., Ziervogel, K., MacGregor, B., Teske, A. & Arnosti, C. (2014) Composition and enzymatic function of particle-associated and free-living bacteria: a coastal/offshore comparison. *The ISME Journal*, 8, 2167–2179.

Davies, G. & Henrissat, B. (1995) Structures and mechanisms of glycosyl hydrolases. *Structure*, 3, 853–859.

De Santi, C., Gani, O.A., Helland, R. & Williamson, A. (2017) Structural insight into a CE15 esterase from the marine bacterial metagenome. *Scientific Reports*, 7, 17278.

Deniaud, E., Quemener, B., Fleurence, J. & Lahaye, M. (2003) Structural studies of the mix-linked β-(1→3)/β-(1→4)-d-xylans from the cell wall of *Palmaria palmata* (Rhodophyta). *International Journal of Biological Macromolecules*, 33, 9–18.

Ebringerová, A. (2005) Structural diversity and application potential of hemicelluloses. *Macromolecular Symposia*, 232, 1–12.

Ferreira, L.M.A., Durrant, A.J., Hall, J., Hazlewood, G.P. & Gilbert, H. J. (1990) Spatial separation of protein domains is not necessary for catalytic activity or substrate binding in a xylanase. *The Biochemical Journal*, 269, 261–264.

Ficko-Blean, E., Préchoux, A., Thomas, F., Rochat, T., Larocque, R., Zhu, Y. et al. (2017) Carrageenan catabolism is encoded by a complex regulon in marine heterotrophic bacteria. *Nature Communications*, 8, 1685.

Field, C.B. (1998) Primary production of the biosphere: integrating terrestrial and oceanic components. *Science*, 281, 237–240.

Filippini, M., Kaech, A., Ziegler, U. & Bagheri, H.C. (2011) *Fibrisoma limi* gen. nov., sp. nov., a filamentous bacterium isolated from tidal flats. *International Journal of Systematic and Evolutionary Microbiology*, 61, 1418–1424.

Filippini, M., Svercel, M., Laczko, E., Kaech, A., Ziegler, U. & Bagheri, H.C. (2011) *Fibrella aestuarina* gen. nov., sp. nov., a filamentous bacterium of the family Cytophagaceae isolated from a tidal flat, and emended description of the genus Rudanella Weon et al. 2008. *International Journal of Systematic and Evolutionary Microbiology*, 61, 184–189.

Finn, R.D., Clements, J. & Eddy, S.R. (2011) HMMER web server: interactive sequence similarity searching. *Nucleic Acids Research*, 39, W29–W37.

Francis, T.B., Bartosik, D., Sura, T., Sichert, A., Hehemann, J.-H., Markert, S. et al. (2021) Changing expression patterns of TonB-dependent transporters suggest shifts in polysaccharide consumption over the course of a spring phytoplankton bloom. *The ISME Journal*, 15, 2336–2350.

Gilbert, H.J. (2010) The biochemistry and structural biology of plant cell wall deconstruction. *Plant Physiology*, 153, 444–455.

Gilbert, H.J. & Hazlewood, G.P. (1993) Bacterial cellulases and xylanases. *Journal of General Microbiology*, 139, 187–194.

Gilbert, H.J., Hazlewood, G.P., Laurie, J.I., Orpin, C.G. & Xue, G.P. (1992) Homologous catalytic domains in a rumen fungal xylanase: evidence for gene duplication and prokaryotic origin. *Molecular Microbiology*, 6, 2065–2072.

Gilchrist, C.L.M., Booth, T.J., van Wersch, B., van Grieken, L., Medema, M.H. & Chooi, Y.-H. (2021) cblaster: a remote search tool for rapid identification and visualization of homologous gene clusters. *Bioinformatics Advances*, 1, vbab016.

Glenwright, A.J., Pothula, K.R., Bhamidimarri, S.P., Chorev, D.S., Baslé, A., Firbank, S.J. et al. (2017) Structural basis for nutrient acquisition by dominant members of the human gut microbiota. *Nature*, 541, 407–411.

Gloster, T.M., Williams, S.J., Roberts, S., Tarling, C.A., Wicki, J., Withers, S.G. et al. (2004) Atomic resolution analyses of the binding of xylobiose-derived deoxynojirimycin and isofagomine to xylanase Xyn10A. *Chemical Communications*, *16*, 1794.

Gray, D.A., White, J.B.R., Oluwole, A.O., Rath, P., Glenwright, A.J., Mazur, A. et al. (2021) Insights into SusCD-mediated glycan import by a prominent gut symbiont. *Nature Communications*, 12, 44.

Guindon, S., Dufayard, J.-F., Lefort, V., Anisimova, M., Hordijk, W. & Gascuel, O. (2010) New algorithms and methods to estimate maximum-likelihood phylogenies: assessing the performance of PhyML 3.0. *Systematic Biology*, 59, 307–321.

Hao, Z., Lv, D., Ge, Y., Shi, J., Weijers, D., Yu, G. et al. (2020) *RIdeogram*: drawing SVG graphics to visualize and map genome-wide data on the idiograms. *PeerJ Computer Science*, 6, e251.

Hehemann, J.-H., Boraston, A.B. & Czjzek, M. (2014) A sweet new wave: structures and mechanisms of enzymes that digest polysaccharides from marine algae. *Current Opinion in Structural Biology*, 28, 77–86.

Hehemann, J.-H., Correc, G., Barbeyron, T., Helbert, W., Czjzek, M. & Michel, G. (2010) Transfer of carbohydrate-active enzymes from marine bacteria to Japanese gut microbiota. *Nature*, 464, 908–912.

Hehemann, J.-H., Kelly, A.G., Pudlo, N.A., Martens, E.C. & Boraston, A.B. (2012) Bacteria of the human gut microbiome catabolize red seaweed glycans with carbohydrate-active enzyme updates from extrinsic microbes. *Proceedings of the National Academy of Sciences*, 109, 19786–19791.

Hemingway, J.D., Schefuß, E., Spencer, R.G.M., Dinga, B.J., Eglinton, T.I., McIntyre, C. et al. (2017) Hydrologic controls on seasonal and inter-annual variability of Congo River particulate organic matter source and reservoir age. *Chemical Geology*, 466, 454–465.

Herrmann, N., Boom, A., Carr, A.S., Chase, B.M., Granger, R., Hahn, A. et al. (2016) Sources, transport and deposition of terrestrial organic material: a case study from southwestern Africa. *Quaternary Science Reviews*, 149, 215–229.

Hettiarachchi, S.A., Kwon, Y.-K., Lee, Y., Jo, E., Eom, T.-Y., Kang, Y.-H. et al. (2019) Characterization of an acetyl xylan esterase from the marine bacterium *Ochrovirga pacifica* and its synergism with xylanase on beechwood xylan. *Microbial Cell Factories*, 18, 122.

Hoagland, K.D., Rosowski, J.R., Gretz, M.R. & Roemer, S.C. (1993) Diatom extracellular polymeric substances: functions, fine structure, chemistry, and physiology. *Journal of Phycology*, 29, 537–566.

Hsieh, Y.J. & Harris, P. (2019) Xylans of red and green algae: what is known about their structures and how they are synthesised? *Polymers*, 11, 354.

Huang, G., Vidal-Melgosa, S., Sichert, A., Becker, S., Fang, Y., Niggemann, J. et al. (2021) Secretion of sulfated fucans by diatoms may contribute to marine aggregate formation. *Limnology and Oceanography*, 66, 3768–3782.

Jensen, J.K., Busse-Wicher, M., Poulsen, C.P., Fangel, J.U., Smith, P.J., Yang, J.-Y. et al. (2018) Identification of an algal xylan synthase indicates that there is functional orthology between algal and plant cell wall biosynthesis. *The New Phytologist*, 218, 1049–1060.

Kappelmann, L., Krüger, K., Hehemann, J.-H., Harder, J., Markert, S., Unfried, F. et al. (2019) Polysaccharide utilization loci of North Sea Flavobacteriia as basis for using SusC/D-protein expression for predicting major phytoplankton glycans. *The ISME Journal*, 13, 76–91.

Klemetsen, T., Raknes, I.A., Fu, J., Agafonov, A., Balasundaram, S. V., Tartari, G. et al. (2018) The MAR databases: development and implementation of databases specific for marine metagenomics. *Nucleic Acids Research*, 46, D692–D699.

Kloareg, B. & Quatrano, R.S. (1988) Structure of the cell walls of marine algae and ecophysiological functions of the matrix

polysaccharides. *Oceanography and Marine Biology: An Annual Review*, 26, 259–315.

Kmezik, C., Krska, D., Mazurkewich, S. & Larsbrink, J. (2021) Characterization of a novel multidomain CE15-GH8 enzyme encoded by a polysaccharide utilization locus in the human gut bacterium *Bacteroides eggerthii*. *Scientific Reports*, 11, 17662.

Koropatkin, N.M., Martens, E.C., Gordon, J.I. & Smith, T.J. (2008) Starch catabolism by a prominent human gut symbiont is directed by the recognition of amylose helices. *Structure*, 16, 1105–1115.

Kraan, S. (2012) Algal polysaccharides, novel applications and outlook. In *Carbohydrates—Comprehensive Studies on Glycobiology and Glycotechnology*. London: InTech, pp. 1–44.

Krüger, K., Chafee, M., Ben Francis, T., Glavina del Rio, T., Becher, D., Schweder, T. et al. (2019) In marine *Bacteroidetes* the bulk of glycan degradation during algae blooms is mediated by few clades using a restricted set of genes. *The ISME Journal*, 13, 2800–2816.

Krzywinski, M., Schein, J., Birol, I., Connors, J., Gascoyne, R., Horsman, D. et al. (2009) Circos: an information aesthetic for comparative genomics. *Genome Research*, 19, 1639–1645.

Lahaye, M., Rondeau-Mouro, C., Deniaud, E. & Buléon, A. (2003) Solid-state 13C NMR spectroscopy studies of xylans in the cell wall of *Palmaria palmata*. *Carbohydrate Research*, 338, 1559–1569.

Larsbrink, J., Rogers, T.E., Hemsworth, G.R., McKee, L.S., Tauzin, A.S., Spadiut, O. et al. (2014) A discrete genetic locus confers xyloglucan metabolism in select human gut Bacteroidetes. *Nature*, 506, 498–502.

Larsbrink, J., Thompson, A.J., Lundqvist, M., Gardner, J.G., Davies, G.J. & Brumer, H. (2014) A complex gene locus enables xyloglucan utilization in the model saprophyte *C ellvibrio japonicus*: *Cellvibrio japonicus* xyloglucan utilization locus. *Molecular Microbiology*, 94, 418–433.

Letunic, I. & Bork, P. (2021) Interactive Tree Of Life (iTOL) v5: an online tool for phylogenetic tree display and annotation. *Nucleic Acids Research*, 49, W293–W296.

Lex, A., Gehlenborg, N., Strobelt, H., Vuillemot, R. & Pfister, H. (2014) UpSet: visualization of intersecting sets. *IEEE Transactions on Visualization and Computer Graphics*, 20, 1983–1992.

Li, C., Wen, A., Shen, B., Lu, J., Huang, Y. & Chang, Y. (2011) FastCloning: a highly simplified, purification-free, sequence- and ligation-independent PCR cloning method. *BMC Biotechnology*, 11, 92.

Lombard, V., Golaconda Ramulu, H., Drula, E., Coutinho, P.M. & Henrissat, B. (2014) The carbohydrate-active enzymes database (CAZy) in 2013. *Nucleic Acids Research*, 42, D490–D495.

Mackie, I.M. & Percival, E. (1959) The constitution of xylan from the green seaweed *Caulerpa filiformis*. *Journal of the Chemical Society Resumed*, 1, 1151–1156.

Martens, E.C., Koropatkin, N.M., Smith, T.J. & Gordon, J.I. (2009) Complex glycan catabolism by the human gut microbiota: the *Bacteroidetes* Sus-like paradigm. *The Journal of Biological Chemistry*, 284, 24673–24677.

Martone, P.T., Estevez, J.M., Lu, F., Ruel, K., Denny, M.W., Somerville, C. et al. (2009) Discovery of lignin in seaweed reveals convergent evolution of cell-wall architecture. *Current Biology*, 19, 169–175.

McKee, L.S., La Rosa, S.L., Westereng, B., Eijsink, V.G., Pope, P. B. & Larsbrink, J. (2021) Polysaccharide degradation by the *Bacteroidetes*: mechanisms and nomenclature. *Environmental Microbiology Reports*, 13, 559–581.

Notenboom, V., Boraston, A.B., Kilburn, D.G. & Rose, D.R. (2001) Crystal structures of the family 9 carbohydrate-binding module from *Thermotoga maritima* xylanase 10A in native and ligand-bound forms. *Biochemistry*, 40, 6248–6256.

Opsahl, S. & Benner, R. (1997) Distribution and cycling of terrigenous dissolved organic matter in the ocean. *Nature*, 386, 480–482.

Otto, A., Bernhardt, J., Meyer, H., Schaffer, M., Herbst, F.-A., Siebourg, J. et al. (2010) Systems-wide temporal proteomic profiling in glucose-starved *Bacillus subtilis*. *Nature Communications*, 1, 137.

Pell, G., Taylor, E.J., Gloster, T.M., Turkenburg, J.P., Fontes, C.M.G. A., Ferreira, L.M.A. et al. (2004) The mechanisms by which family 10 glycoside hydrolases bind decorated substrates. *The Journal of Biological Chemistry*, 279, 9597–9605.

Pereira, G.V., Abdel-Hamid, A.M., Dutta, S., D'Alessandro-Gabazza, C.N., Wefers, D., Farris, J.A. et al. (2021) Degradation of complex arabinoxylans by human colonic *Bacteroidetes*. *Nature Communications*, 12, 459.

Perez-Riverol, Y., Bai, J., Bandla, C., García-Seisdedos, D., Hewapathirana, S., Kamatchinathan, S. et al. (2021) The PRIDE database resources in 2022: a hub for mass spectrometry-based proteomics evidences. *Nucleic Acids Research*, 50, D543–D552.

Peterson, B.J., Holmes, R.M., McClelland, J.W., Vörösmarty, C.J., Lammers, R.B., Shiklomanov, A.I. et al. (2002) Increasing river discharge to the Arctic ocean. *Science*, 298, 2171–2173.

Pollet, R.M., Martin, L.M. & Koropatkin, N.M. (2021) TonB-dependent transporters in the Bacteroidetes: unique domain structures and potential functions. *Molecular Microbiology*, 115, 490–501.

Popper, Z.A., Michel, G., Hervé, C., Domozych, D.S., Willats, W.G.T., Tuohy, M.G. et al. (2011) Evolution and diversity of plant cell walls: from algae to flowering plants. *Annual Review of Plant Biology*, 62, 567–590.

Raymond, P.A., McClelland, J.W., Holmes, R.M., Zhulidov, A.V., Mull, K., Peterson, B.J. et al. (2007) Flux and age of dissolved organic carbon exported to the Arctic Ocean: A carbon isotopic study of the five largest arctic rivers: ARCTIC RIVER DOC. *Global Biogeochemical Cycles*, 21.

Reintjes, G., Arnosti, C., Fuchs, B.M. & Amann, R. (2017) An alternative polysaccharide uptake mechanism of marine bacteria. *The ISME Journal*, 11, 1640–1650.

Reisky, L., Préchoux, A., Zühlke, M.-K., Bäumgen, M., Robb, C.S., Gerlach, N. et al. (2019) A marine bacterial enzymatic cascade degrades the algal polysaccharide ulvan. *Nature Chemical Biology*, 15, 803–812.

Repeta, D.J. & Aluwihare, L.I. (2006) Radiocarbon analysis of neutral sugars in high-molecular-weight dissolved organic carbon: implications for organic carbon cycling. *Limnology and Oceanography*, 51, 1045–1053.

Robb, C.S., Hobbs, J.K., Pluvinage, B., Reintjes, G., Klassen, L., Monteith, S. et al. (2022) Metabolism of a hybrid algal galactan by members of the human gut microbiome. *Nature Chemical Biology*, 18, 501–510.

Rogowski, A., Briggs, J.A., Mortimer, J.C., Tryfona, T., Terrapon, N., Lowe, E.C. et al. (2015) Glycan complexity dictates microbial resource allocation in the large intestine. *Nature Communications*, 6, 7481.

Salmeán, A.A., Willats, W.G.T., Ribeiro, S., Andersen, T.J. & Ellegaard, M. (2022) Over 100-year preservation and temporal fluctuations of cell wall polysaccharides in marine sediments. *Frontiers in Plant Science*, 13, 785902.

Sayers, E.W., Bolton, E.E., Brister, J.R., Canese, K., Chan, J., Comeau, D.C. et al. (2022) Database resources of the national center for biotechnology information. *Nucleic Acids Research*, 50, D20–D26.

Schefuß, E., Schouten, S. & Schneider, R.R. (2005) Climatic controls on central African hydrology during the past 20,000 years. *Nature*, 437, 1003–1006.

Schut, F., de Vries, E.J., Gottschal, J.C., Robertson, B.R., Harder, W., Prins, R.A. et al. (1993) Isolation of typical marine bacteria by dilution culture: growth, maintenance, and characteristics of isolates under laboratory conditions. *Applied and Environmental Microbiology*, 59, 2150–2160.

Shogren, A.J., Zarnetske, J.P., Abbott, B.W., Iannucci, F., Medvedeff, A., Cairns, S. et al. (2021) Arctic concentration–

discharge relationships for dissolved organic carbon and nitrate vary with landscape and season. *Limnology and Oceanography*, 66, 197–215.

Starr, C.M., Irene Masada, R., Hague, C., Skop, E. & Klock, J.C. (1996) Fluorophore-assisted carbohydrate electrophoresis in the separation, analysis, and sequencing of carbohydrates. *Journal of Chromatography. A*, 720, 295–321.

Tauzin, A.S., Kwiatkowski, K.J., Orlovsky, N.I., Smith, C.J., Creagh, A.L., Haynes, C.A. et al. (2016) Molecular dissection of xyloglucan recognition in a prominent human gut symbiont. *MBio*, 7, e02134-15.

Teeling, H., Fuchs, B.M., Becher, D., Klockow, C., Gardebrecht, A., Bennke, C.M. et al. (2012) Substrate-controlled succession of marine bacterioplankton populations induced by a phytoplankton bloom. *Science*, 336, 608–611.

Teufel, F., Almagro Armenteros, J.J., Johansen, A.R., Gíslason, M.H., Pihl, S.I., Tsirigos, K.D. et al. (2022) SignalP 6.0 predicts all five types of signal peptides using protein language models. *Nature Biotechnology*, 40, 1023–1025.

The Human Microbiome Project Consortium. (2012a) A framework for human microbiome research. *Nature*, 486, 215–221.

The Human Microbiome Project Consortium. (2012b) Structure, function and diversity of the healthy human microbiome. *Nature*, 486, 207–214.

Thompson, J.D., Higgins, D.G. & Gibson, T.J. (1994) CLUSTAL W: improving the sensitivity of progressive multiple sequence alignment through sequence weighting, position-specific gap penalties and weight matrix choice. *Nucleic Acids Research*, 22, 4673–4680.

Tranvik, L.J. & Jansson, M. (2002) Terrestrial export of organic carbon. *Nature*, 415, 861–862.

Tull, D. & Withers, S.G. (1994) Mechanisms of cellulases and xylanases: a detailed kinetic study of the exo-.beta.-1,4-glycanase from *Cellulomonas Fimi*. *Biochemistry*, 33, 6363–6370.

Unfried, F., Becker, S., Robb, C.S., Hehemann, J.-H., Markert, S., Heiden, S.E. et al. (2018) Adaptive mechanisms that provide competitive advantages to marine bacteroidetes during microalgal blooms. *The ISME Journal*, 12, 2894–2906.

Viana, A.G., Noseda, M.D., Gonçalves, A.G., Duarte, M.E.R., Yokoya, N., Matulewicz, M.C. et al. (2011) β-d-(1→4), β-d-(1→3) 'mixed linkage' xylans from red seaweeds of the order Nemaliales and Palmariales. *Carbohydrate Research*, 346, 1023–1028.

Vidal-Melgosa, S., Lagator, M., Sichert, A., Priest, T., Pätzold, J. & Hehemann, J.-H. (2022) Not digested: algal glycans move carbon dioxide into the deep-sea. *Preprint*. https://doi.org/10.1101/2022.03.04.483023

Vidal-Melgosa, S., Sichert, A., Francis, T.B., Bartosik, D., Niggemann, J., Wichels, A. et al. (2021) Diatom fucan polysaccharide precipitates carbon during algal blooms. *Nature Communications*, 12, 1150.

Williamson, G., Kroon, P. & Faulds, C. (1998) Hairy plant polysaccharides: a close shave with microbial esterases. *Microbiology (Reading, England)*, 144(Pt 8), 2011–2023.

Wong, T., Brault, L., Gasparotto, E., Vallée, R., Morvan, P.-Y., Ferrières, V. et al. (2021) Formation of amphiphilic molecules from the most common marine polysaccharides, toward a sustainable alternative? *Molecules*, 26, 4445.

Yeh, Y.-C. & Fuhrman, J.A. (2022) Effects of phytoplankton, viral communities, and warming on free-living and particle-associated marine prokaryotic community structure. *Nature Communications*, 13, 7905.

Zhang, H., Yohe, T., Huang, L., Entwistle, S., Wu, P., Yang, Z. et al. (2018) dbCAN2: a meta server for automated carbohydrate-active enzyme annotation. *Nucleic Acids Research*, 46, W95–W101.

SUPPORTING INFORMATION

Additional supporting information can be found online in the Supporting Information section at the end of this article.

How to cite this article: Dutschei, T., Beidler, I., Bartosik, D., Seeßelberg, J.-M., Teune, M., Bäumgen, M. et al. (2023) Marine *Bacteroidetes* enzymatically digest xylans from terrestrial plants. *Environmental Microbiology*, 25(9), 1713–1727. Available from: https://doi.org/10.1111/1462-2920.16390